

**Jalal M. Jalil** 

Electromechanical Engineering  
Department, University of  
Technology, Baghdad, Iraq.  
[jalalmjalil@yahoo.com](mailto:jalalmjalil@yahoo.com)

**Ghaydaa K. Salih**

Electromechanical Engineering  
Department, University of  
Technology, Baghdad, Iraq.  
[g\\_kaain@yahoo.com](mailto:g_kaain@yahoo.com)

**Yosif A. Madhi**

Electromechanical Engineering  
Department, University of  
Technology, Baghdad, Iraq.  
[joealmiahi55@gmail.com](mailto:joealmiahi55@gmail.com)

Received on: 30/08/2017  
Accepted on: 25/01/2018  
Published online: 25/8/2018

## Performance Study of Solar Air Heater with Thermally Conducted Multi V Shaped Baffles and Ribs

**Abstract-** In this study, solar air heater with thermally conducted multi V shaped baffles and with same baffles and ribs are investigated experimentally and numerically to improve the performance of conventional air heaters. Numerically, steady state 3D forced convection turbulent model is used to solve Navier Stokes and energy equations of airflow inside rectangular duct of solar air heater. The code was validated by comparing the numerical result with experimental results and the agreement seems acceptable. The numerical studies were extended to study the cases of flat plate and straight baffles solar air heater. From experimental and numerical studies, it was found that the collector with V shaped baffles and ribs has the highest efficiency. The results showed that the V shaped baffles and ribs solar air heater is 14% more efficient compared to flat plate collectors.

**Keywords-** Solar air heater, CFD, Effective efficiency.

**How to cite this article:** J.M. Jalil, G.K. Salih and Y.A. Madhi, "Performance Study of Solar Air Heater with Thermally Conducted Multi V Shaped Baffles and Ribs," *Engineering and Technology Journal*, Vol. 36, Part A, No. 8, pp. 930-938, 2018.

### 1. Introduction

Solar air heater is simple thermal system used for low temperature heating. A transparent material sheet such as plastic or glass is fixed above the absorber plate and the system is insulated thermally from the back and from the sides [1]. The solar air heater is widely used for domestic space heating and crop drying (grains, fruit, vegetables, etc.). The main disadvantage is low thermal efficiency because of low heat capacity and low thermal conductivity of the air. Many researchers tried to increase the efficiency of solar air heaters through supplying an intimate heat transfer between air and absorbing plate. With improvements in design and manufacturing materials which lead to higher efficiency and low cost, solar air heaters can find new application in industry such as (1) Air pre-heating for combustion processes. (2) Drying minerals, coal, paper. (3) Space heating for warehouses, factories. To make a solar air heater more effective solar energy utilization system, thermal efficiency needs to be improved by enhancing heat transfer rate. To accomplish that, heat has to be transferred efficiently from the absorber to the flowing air. This will decrease absorber plate temperature and thus minimize convection and radiation losses through the glass. The performance of solar air heater was studied widely in recent years. Several technicalities were

<https://doi.org/10.30684/etj.36.8A.14>

2412-0758/University of Technology-Iraq, Baghdad, Iraq

This is an open access article under the CC BY 4.0 license <http://creativecommons.org/licenses/by/4.0>

used to estimate the thermo-hydraulic performance of solar air heater. Karwa et al. [2] investigated the performance of solar air heaters with chamfered rib-roughness on the absorber plates. Aharwal et al. [3] examine a rectangular duct roughened with square rib split with a gap arranged at an inclination with direction of flow. Lanjewar et al. [4] studied experimentally W shaped ribs on absorber plate with two arrangements downstream and upstream to the flow. Pottler et al. [5] stated that offset strip fins do not show an improved performance when compared to optimally spaced continuous fins, due to the fan power losses for this geometry. Priyam and Chand [6] evaluated analytically the performance of solar air heater with two transverse wavy fins. Falih [7] found that the inclined baffles with baffle pitch to duct height ratio of 1 gives higher heat transfer rate than the one with ratio of 2 and the smooth duct respectively, and the highest heat transfer and pressure drop is found by using baffle with 30°. Chamoli and Thakur [8] studied the performance of solar air heaters roughened with V down perforated baffles. Their Investigations have been performed using a mathematical model to study the effects of ambient conditions, operating and design on the effective efficiency. Kumar et al. [9] deal with broken multiple V-type baffles. The results revealed that the broken multiple V-type

baffles are thermo-hydraulically superior as compared to the other baffles. Kumar and Kim [10] showed that multi V-type perforated baffles performed better as compared to other shapes baffle in a rectangular duct. Karim and Hawlader [11], investigated flat plate, finned and V-corrugated solar air heaters. The V-corrugated collector was found to be the most efficient collector and the flat plate collector to be the least efficient. In this work, solar air heater with baffles and ribs has been investigated numerically and experimentally. The effect of baffles and ribs on fluid flow and heat transfer has been studied and analyzed.

## 2. Mathematical Model

### I. Governing Equations

The governing equations are continuity, Navier Stokes and energy equations [12]:

$$\frac{\partial U}{\partial x} + \frac{\partial V}{\partial y} + \frac{\partial W}{\partial z} = 0 \quad (1)$$

$$\frac{\partial U^2}{\partial x} + \frac{\partial UV}{\partial y} + \frac{\partial UW}{\partial z} = -\frac{1}{\rho} \frac{\partial P}{\partial x} + \frac{\partial}{\partial x} \left( \nu_e \frac{\partial U}{\partial x} \right) + \frac{\partial}{\partial y} \left( \nu_e \frac{\partial U}{\partial y} \right) + \frac{\partial}{\partial z} \left( \nu_e \frac{\partial U}{\partial z} \right) + \frac{\partial}{\partial x} \left( \nu_e \frac{\partial U}{\partial x} \right) + \frac{\partial}{\partial y} \left( \nu_e \frac{\partial V}{\partial x} \right) + \frac{\partial}{\partial z} \left( \nu_e \frac{\partial W}{\partial x} \right) \quad (2)$$

$$\frac{\partial UV}{\partial x} + \frac{\partial V^2}{\partial y} + \frac{\partial VW}{\partial z} = -\frac{1}{\rho} \frac{\partial P}{\partial y} + \frac{\partial}{\partial x} \left( \nu_e \frac{\partial V}{\partial x} \right) + \frac{\partial}{\partial y} \left( \nu_e \frac{\partial V}{\partial y} \right) + \frac{\partial}{\partial z} \left( \nu_e \frac{\partial V}{\partial z} \right) + \frac{\partial}{\partial x} \left( \nu_e \frac{\partial U}{\partial y} \right) + \frac{\partial}{\partial y} \left( \nu_e \frac{\partial V}{\partial y} \right) + \frac{\partial}{\partial z} \left( \nu_e \frac{\partial W}{\partial y} \right) \quad (3)$$

$$\frac{\partial UW}{\partial x} + \frac{\partial VW}{\partial y} + \frac{\partial W^2}{\partial z} = -\frac{1}{\rho} \frac{\partial P}{\partial z} + \frac{\partial}{\partial x} \left( \nu_e \frac{\partial W}{\partial x} \right) + \frac{\partial}{\partial y} \left( \nu_e \frac{\partial W}{\partial y} \right) + \frac{\partial}{\partial z} \left( \nu_e \frac{\partial W}{\partial z} \right) + \frac{\partial}{\partial x} \left( \nu_e \frac{\partial U}{\partial z} \right) + \frac{\partial}{\partial y} \left( \nu_e \frac{\partial V}{\partial z} \right) + \frac{\partial}{\partial z} \left( \nu_e \frac{\partial W}{\partial z} \right) \quad (4)$$

$$\frac{\partial UT}{\partial x} + \frac{\partial VT}{\partial y} + \frac{\partial WT}{\partial z} = \frac{\partial}{\partial x} \left( \Gamma_e \frac{\partial T}{\partial x} \right) + \frac{\partial}{\partial y} \left( \Gamma_e \frac{\partial T}{\partial y} \right) + \frac{\partial}{\partial z} \left( \Gamma_e \frac{\partial T}{\partial z} \right) \quad (5)$$

To solve the governing Equations (1 to 5), mathematical expressions for effective kinematic viscosity,  $\nu_e$ , and effective diffusion coefficient,  $\Gamma_e$ , are required through use of turbulence model. The standard  $k$ - $\epsilon$  model [13] has two equations, one for  $k$  and one for  $\epsilon$ . It uses the following transport equations for  $k$  and  $\epsilon$ .

$$\frac{\partial}{\partial x} (kU) + \frac{\partial}{\partial y} (kV) + \frac{\partial}{\partial z} (kW) = \frac{\partial}{\partial x} \left( \frac{\nu_t}{\sigma_k} \frac{\partial k}{\partial x} \right) + \frac{\partial}{\partial y} \left( \frac{\nu_t}{\sigma_k} \frac{\partial k}{\partial y} \right) + \frac{\partial}{\partial z} \left( \frac{\nu_t}{\sigma_k} \frac{\partial k}{\partial z} \right) + G - \epsilon \quad (6)$$

$$\frac{\partial}{\partial x} (\epsilon U) + \frac{\partial}{\partial y} (\epsilon V) + \frac{\partial}{\partial z} (\epsilon W) = \frac{\partial}{\partial x} \left( \frac{\nu_t}{\sigma_\epsilon} \frac{\partial k}{\partial x} \right) + \frac{\partial}{\partial y} \left( \frac{\nu_t}{\sigma_\epsilon} \frac{\partial k}{\partial y} \right) + \frac{\partial}{\partial z} \left( \frac{\nu_t}{\sigma_\epsilon} \frac{\partial k}{\partial z} \right) + C_{1\epsilon} \frac{\epsilon}{k} G - C_{2\epsilon} \frac{\epsilon^2}{k} \quad (7)$$

$$G = \nu_t \left[ 2 \left( \frac{\partial U}{\partial x} \right)^2 + 2 \left( \frac{\partial V}{\partial y} \right)^2 + 2 \left( \frac{\partial W}{\partial z} \right)^2 + \left( \frac{\partial U}{\partial y} + \frac{\partial V}{\partial x} \right)^2 + \left( \frac{\partial V}{\partial z} + \frac{\partial W}{\partial y} \right)^2 + \left( \frac{\partial U}{\partial z} + \frac{\partial W}{\partial x} \right)^2 \right] \quad (8)$$

Where  $\epsilon$ , is the dissipation term. The parametric values in this study are given in Table 1. Numerical procedure called SIMPLE is used to solve the basic governing equations by using a hybrid scheme [14]. The finite volume mesh consists of many control volume using a staggered grid system. The simulations were conducted employing Fortran 90 language and the graphs were plotted using Tec plot. The accuracy of numerical solution is  $5 \times 10^{-3}$  for the present study that is reached at approximately  $6 \times 10^3$  iteration.

### II. Boundary Conditions

Four cases of solar air heater have been simulated which are, flat plate absorber plate, straight baffles, multi-V shape baffles, multi-V shape baffles and ribs. The dimensions of the duct, baffles and ribs in numerical and experimental parts are quite similar and shown in Figure 1. Figure 2 shows the schematic diagram and boundary conditions of the numerical model. The sides and bottom walls are insulated while the temperature of upper wall (absorber plate) is calculated by steady state three-dimension model. Energy balance method, which can be described as the summation of heat in and out equals to zero including solar term, are applied over small elements of six faces to calculate the temperature of absorber plate.

### 3. Experiment Apparatus

The experiments were conducted indoor to maintain the radiation intensity and air temperature. So, bias results caused by different

$C_{\mu}$	$C_{1\epsilon}$	$C_{2\epsilon}$	$\sigma_k$	$\sigma_\epsilon$
0.09	1.44	1.92	1.00	1.30

outdoor condition could be avoided. A schematic diagram of the experimental apparatus and cross section of the collector is shown in Figure 3.

**Table 1: Empirical constants in the  $k$ - $\epsilon$ [13]**

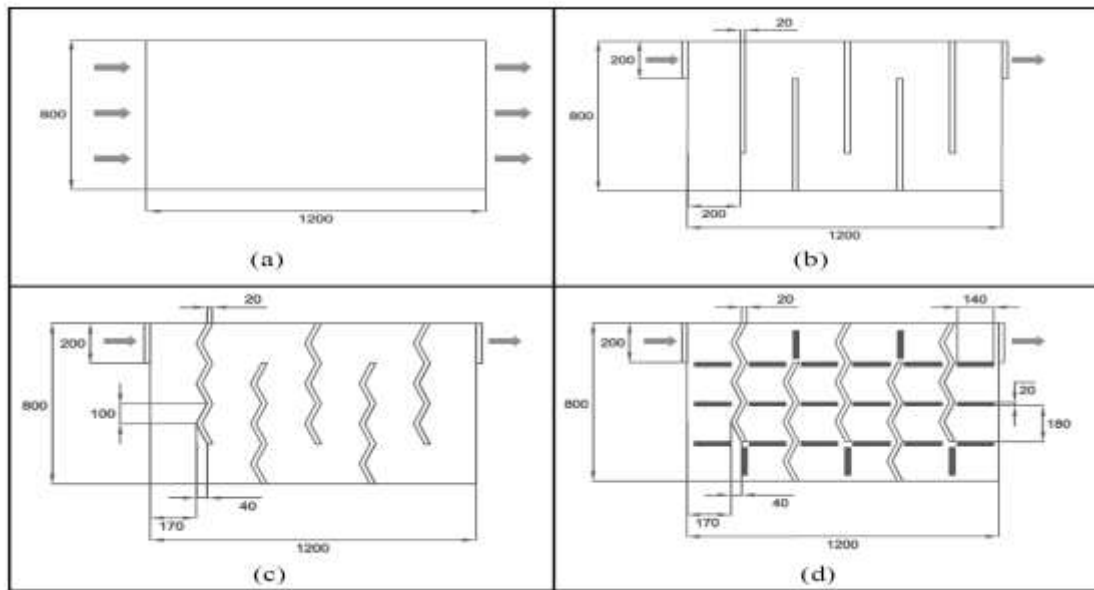


Figure 1: Upper view of collectors with dimensions for numerical and experimental models and directions of flowing air at inlet and outlet for a) smooth absorber plate b) straight baffles c) V shaped baffles d) V shaped baffles and ribs

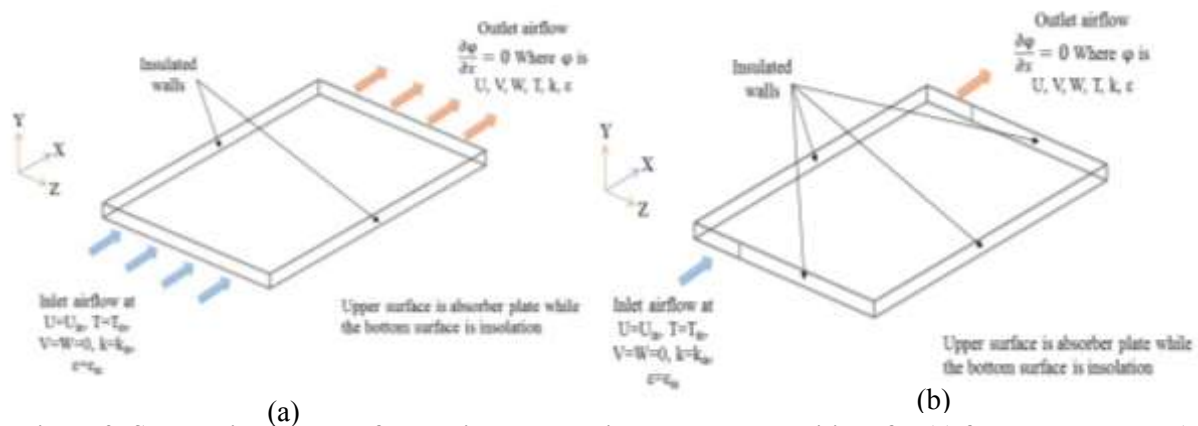


Figure 2: Schematic diagram of numerical model with boundary conditions for (a) flat plate collector (b) other three cases.

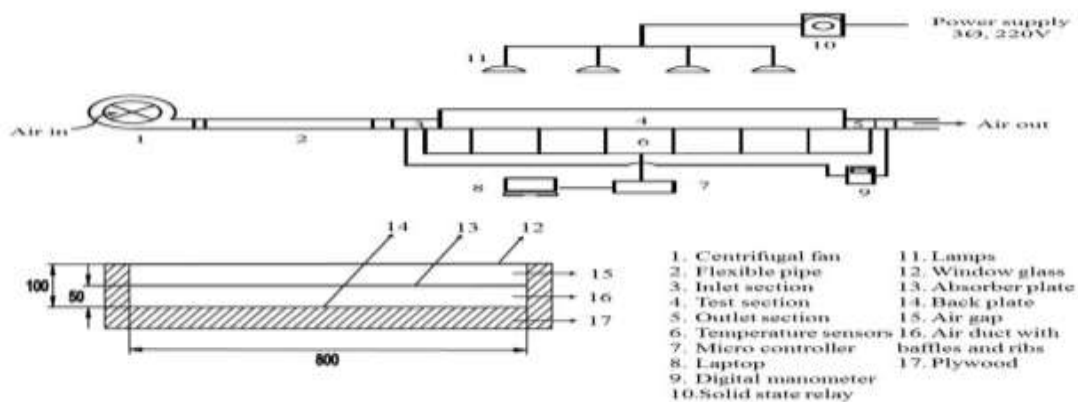


Figure 3: Schematic drawing of the overall experimental system and cross section of the collector

The air was the working medium and was supplied by (0.35) kW centrifugal fan. In operation, this fan which capable of delivering

(390) m<sup>3</sup>/h, pulled air through the collector. The flow rate was changed by controlling the inlet apertures of the fan. A connection hose joins

blower to the collector. At the end of the test duct, the air was exhausted to the atmosphere. The rectangular duct of plywood (represents the insulation of the sides and bottom) has an internal size of 1200\*800\*50 mm. A 1.5 mm-thick galvanized iron plate black matt painted is used as the top wall of the duct. Full height multi V shaped thermally conducted baffles of the same material welded on the lower surface of the absorber plate. The experiment is done in two cases with ribs and without ribs, the arrangement of these two cases is shown in Figure 1 (c and d). The cases of smooth absorber plate and straight baffles shown in Figure 1 (a, b) is just simulated numerically. Plexiglas is used as ribs material. Ribs have 90° angle with airflow 10 mm height, 20 mm width. The airflow generated by the fan enters the collector then the flow takes the shape of the passage formed by the baffles. The absorber plate is heated from the top by supplying variable radiative heat flux by means of sun simulator. The absorber plate is covered by 4 mm thick normal window glass. Solar simulator is used with ten 500-W tungsten halogen lamps and solid-state voltage regulator. The thermal radiation received by the collector was measured using a pyrometer placed on top of the cover glass. The voltage supplied to the lights can be adjusted using small control circuitry to change the intensity of thermal radiation incident on the collector. The control circuitry consists of solid-state voltage regulator and variable resistance.

#### 4. Physical Model

The useful power of solar air heater can be evaluated using [15]

$$Q_u = \dot{m}c_p(T_o - T_i) \quad (9)$$

Based on Eq. 10, the thermal efficiency of solar air heater can be calculated using

$$\eta_{th} = \frac{\dot{m}c_p(T_o - T_i)}{IA_c} \quad (10)$$

Thermohydraulic performance of solar air heater is evaluated on the basis of effective efficiency and is written as

$$\eta_{eff} = \frac{Q_u - P_m}{IA_c} \quad (11)$$

Where  $P_m$  is the mechanical energy required for air propelling through the duct which given by

$$P_m = \frac{\dot{m}\Delta p}{\rho} \quad (12)$$

#### 5. Results and Discussions

The increase of air temperature through the investigated solar air heater depends on many

factors. The major one is the baffles which work in two different ways, first as extended surface area conducted with absorber plate by welding. This surface area increased in the baffles of V shaped due to longer baffles in the z direction. The second way is the turbulence effect of V shaped baffles which increase the heat transfer. The other factor that increases the air temperature is the existence of ribs. Third factor is the mass flow rate, as the mass flow rate increases, the temperature of absorber plate will decrease through the duct and the losses due to convection and radiation will decrease. Finally, the amount of insolation falls on absorber plate will increase its temperature and the temperature of air consequently.

#### I. Experimental Results

Thirty-two tests were carried out. Two cases (V shaped baffle, V shaped baffle and ribs), four values of air inlet mass flow rates were studied (0.0125, 0.025, 0.0375 and 0.05 kg/s) and four values of insolation (700, 800, 900, 1000 W/m<sup>2</sup>). The hydraulic diameter of the duct is 0.08 m with relative roughness height 0.094. Figure 4-5 show the variation of air temperature difference across the duct with insolation at different values of mass flow rates for solar air heater with baffles and with baffles and ribs respectively. As shown in figures air temperature difference across the duct changes linearly with insolation absorbed by collector and decrease as mass flow rate increase. Existence of ribs increases the temperature difference slightly across the duct.

#### II. Validation of the code

The numerical model was in conditions similar to those of experimental arrangement. Figure 6 compares between experimental and numerical variation of air temperature difference across the duct with insolation at mass flow rate of 0.05 kg/s for solar air heater with multi V shaped baffles and with multi V shaped baffles and ribs. Figures seem good agreement is achieved between the experimental and numerical results.

#### III. Numerical Results

In the numerical part, same cases and physical conditions of experimental part were simulated with two additional cases, which are smooth absorber plate, and straight baffles to compare the enhancement in heat transfer of using multi V shaped baffles. As shown in Figure 7 the use of straight baffles increases the air temperature difference across the duct for all values of mass flow rates while the highest air temperature

difference across the duct appears in the case of V shaped baffles and ribs.

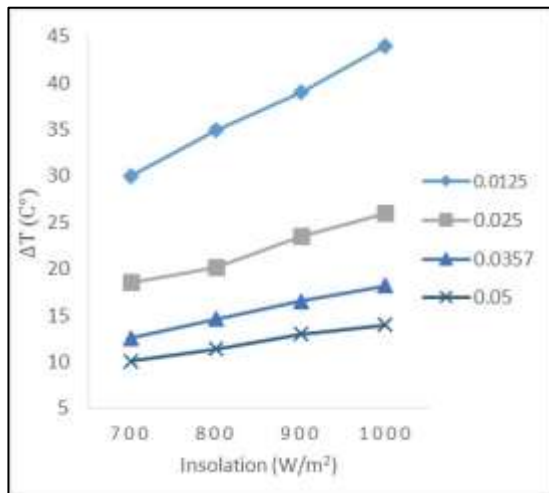


Figure 4: Experimental variation of air temperature difference with insolation at different values of mass flow rate for solar air heater with V shaped baffles

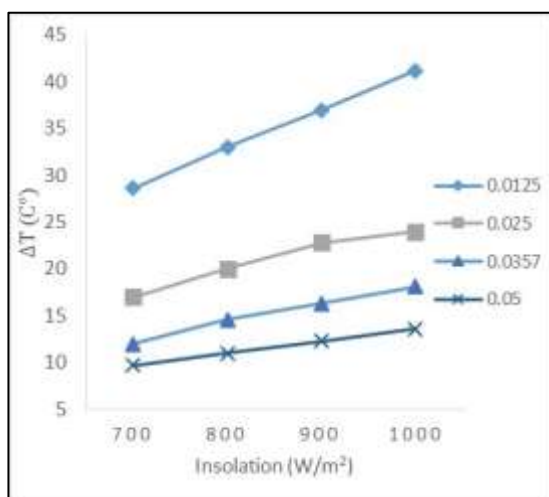


Figure 5: Experimental variation of air temperature difference with insolation at different values of mass flow rate for solar air heater with V shaped baffles and rib

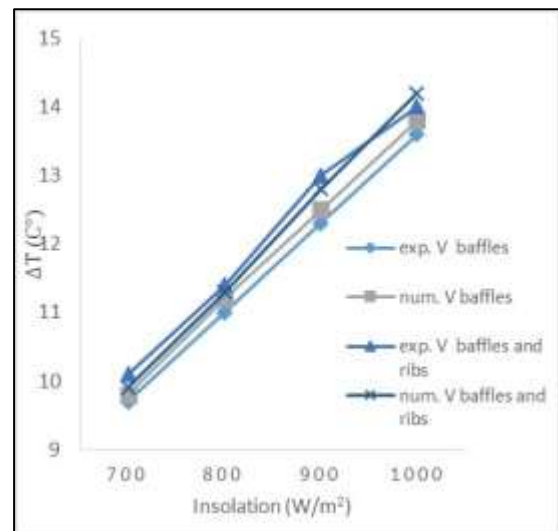


Figure 6: Comparison between experimental and numerical variation of air temperature difference with insolation

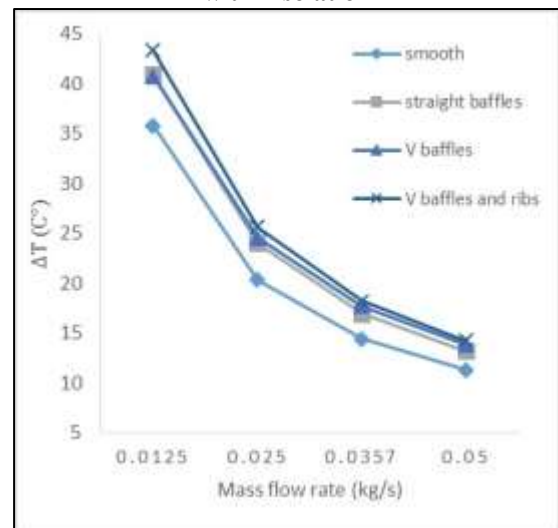


Figure 7: Numerical variation of air temperature difference with mass flow rate for four cases of solar air heater

Figs. 8, 9 and 10 show the velocity vectors for all cases at mass flow rates of 0.05kg/s. Figure 8 shows the formation of a laminar sublayer on smooth absorber plate which represent the main thermal resistance to the heat transferred from the absorber plate to the air flow through the duct. Figure 9 shows the velocity vectors for solar air heater with (a) straight baffles, (b) multi V shaped baffles. It can be seen the creation of back flow adjacent to straight baffles which may cause high-pressure losses.

On the other hand, a circulation is formed near the multi V-shape baffles, which will enhance the heat transfer rate from the baffles to main stream of flowing air without high cost of pressure losses. Figure 10 explains the behavior of flowing air near the rib elements. It can be seen that ribs reduces the cross section causing an acceleration in the main flow around these obstacles. After the

ribs, the sudden expansion leads to a separation zone behind them, after reattachment the pulled flow builds up a new boundary layer. The latter is accelerated by the main flow through shear force. Figure 11 shows the temperature contour (x z plane) at  $y = 0.0375$  m for all cases of solar air heater (a) smooth absorber plate, (b) straight baffles, (c) multi V shaped baffles, (d) multi V shaped baffles and ribs at mass flow rate of 0.05 kg/s and insolation of  $1000 \text{ W/m}^2$ . In the case of smooth absorber plate the temperature of flowing air increases slowly with distance along the duct.

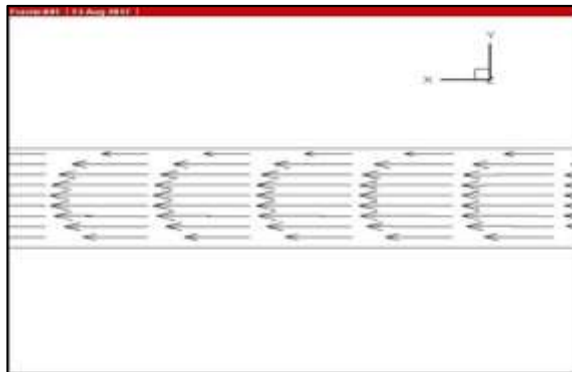


Figure 8: Velocity vector (u and v) at mass flow rate of 0.05 kg/s for smooth absorber plate

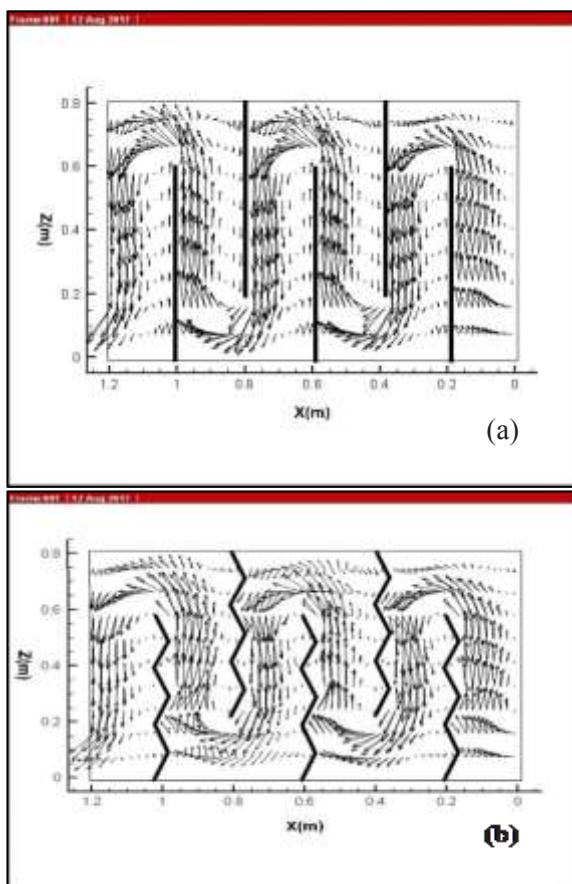


Figure 9: Velocity vector (u and w) at mass flow rate of 0.05 kg/s for a) straight baffles b) V shaped baffles

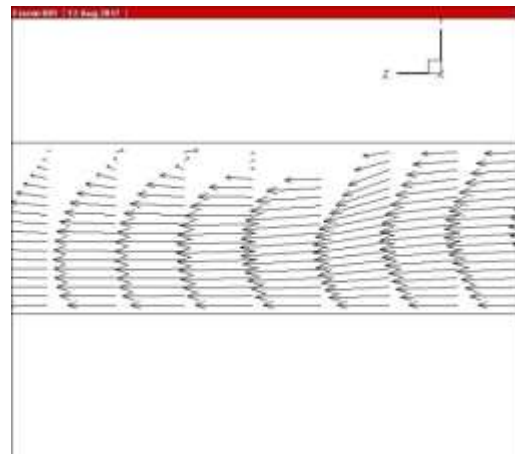


Figure 10: Velocity vector (u and v) at mass flow rate of 0.05 kg/s for V shaped baffles and ribs

The effect of straight baffles on air temperature as heat transfer surface can be seen clearly in the layer adjacent to the baffles. It is clear from this figure that straight baffles have higher temperature than V shaped baffles which can be explained by the high heat transfer coefficient in case of V shaped baffles due to the turbulence effect on the flow and larger surface area exposed to the flowing air. The effect of ribs can be observed by temperature decrease of baffles in case (d) because of decreased temperature of absorber plate due to the effect of ribs on heat transferred from the absorber plate to the airflow. Figure 12 shows the variation of thermal efficiency of four cases tested of solar air heaters as function of mass flow rates and it is found that for the entire range of flow rates the thermal efficiency is higher for straight baffles than smooth absorber plate. The thermal efficiency is increased by using multi V shaped baffles except at mass flow rate of 0.0125 kg/s where it is approximately same as the previous case. The highest thermal efficiency can be obtained by using two different technique (baffles and ribs) which is 77.5% the effect of hydraulic losses caused by baffles and ribs on the performance of solar air heater in term of effective efficiency is shown in Figure 13. An effective performance advantage of 14% in the case of baffles and ribs over the smooth duct solar air heater is obtained. The best effective efficiency obtained for solar air heater is 77.5%.

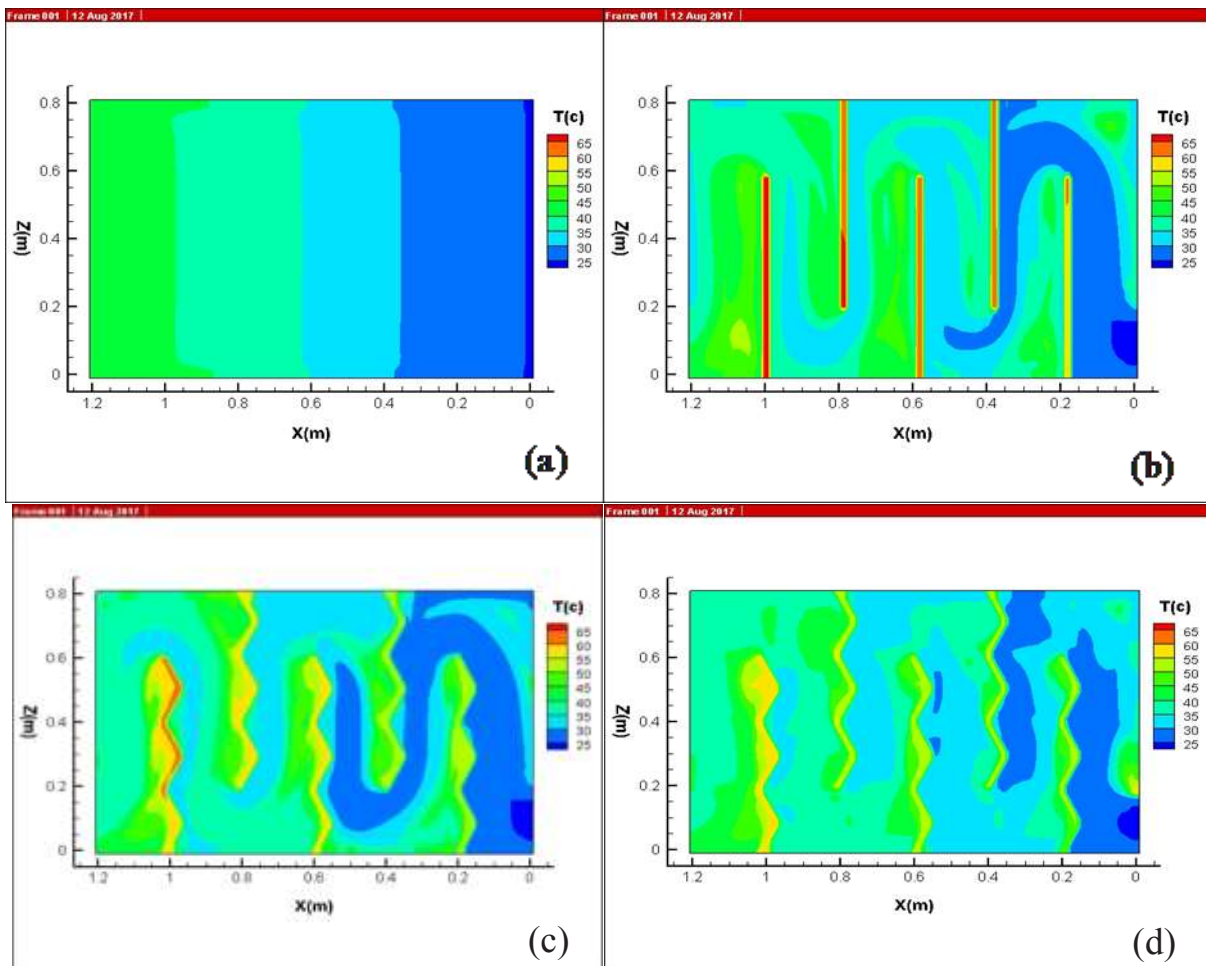


Figure 11: Temperature contour (x z plane) at  $y=0.0375$  m for all cases of solar air heater a) smooth b) straight baffles c) V baffles d) V baffles and ribs

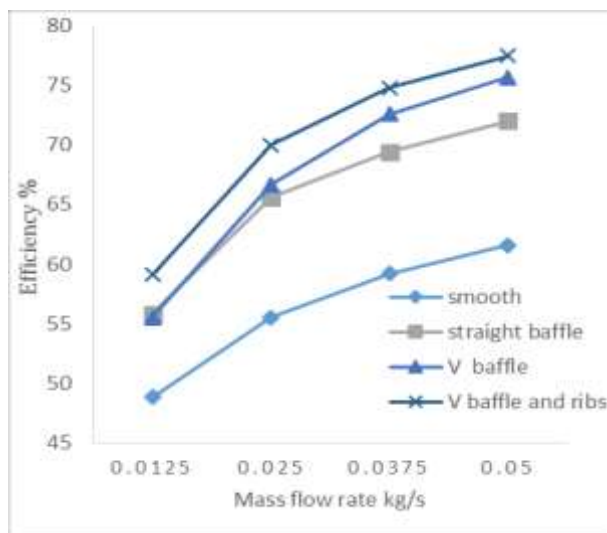


Figure 12: Numerical variation of thermal efficiency as function of mass flow rates for four cases of solar air heater

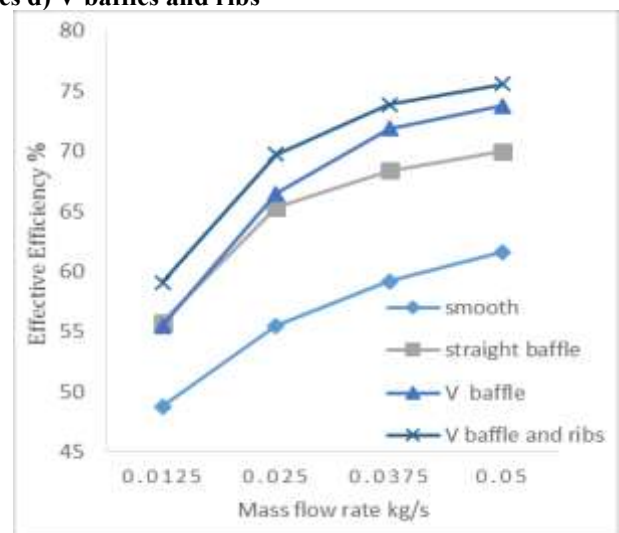


Figure 13: Numerical variation of effective efficiency as function of mass flow rates for four cases of solar air heater

### 3. Conclusions and Recommendations

The following are concluded:

1. Multi V shaped baffles and ribs gains the highest thermal and effective efficiency so it is preferred among the others.
2. Higher air inlet velocity (high Reynolds number) will enhance the thermal and effective performance.
3. Multi V shaped baffles have lower hydraulic losses than straight baffles.
4. Multi V shaped baffles have higher thermal efficiency at high mass flow rates than straight baffles

Based on this work, the following can be recommended for future works:

1. Increase mass flow rate to obtain optimum effective efficiency.
2. Study the effect of the V baffle flexure number and dimensions.
3. Use another arrangement of ribs.

### Nomenclature

#### Symbols

$C_{\mu}$	= Constants in turbulence model
$C_{1\varepsilon}$	
$C_{2\varepsilon}$	
$k$	= Turbulent kinetic energy = $\frac{1}{2}(\mathbf{u}'^2 + \mathbf{v}'^2 + \mathbf{w}'^2)$ $\text{m}^2/\text{s}^2$
$P$	= Mean static pressure, $\text{N}/\text{m}^2$
$T$	= Mean Temperature, $^{\circ}\text{C}$
$U, V, W$	= Dimensionless velocities in X, Y, Z directions, $\text{m}/\text{s}$
$Q_u$	= Useful energy, $\text{W}$
$\dot{m}$	= Mass flow rate, $\text{kg}/\text{s}$
$c_p$	= Specific heat capacity
$T_o$	= Outlet temperature, $^{\circ}\text{C}$
$T_i$	= Inlet temperature, $^{\circ}\text{C}$
$\eta_{th}$	= Thermal efficiency
$I$	= solar radiation, $\text{W}/\text{m}^2$
$A_c$	= Collector area, $\text{m}^2$
$\eta_{eff}$	= Effective efficiency
$p_m$	= Mechanical energy consumption, $\text{W}$
$\Delta p$	= Differential pressure, $\text{pa}$

#### Greek Symbols

$\varepsilon$	= Dissipation rate of turbulent kinetic energy
$\rho$	= Density of air, $\text{kg}/\text{m}^3$
$\sigma_k, \sigma_\varepsilon$	= Turbulent Prandtl numbers for $k, \varepsilon$

$\nu_t$	= Eddy or turbulent viscosity, $\text{m}^2/\text{s}$
$\nu_e$	= Effective kinematics viscosity, $\text{m}^2/\text{s}$
$\Gamma_e$	= Effective diffusion coefficient, $\Gamma = \mu_e / \sigma_e, \text{N.s}/\text{m}^2$
$\phi$	= General dependent variable
$S_\phi$	= Source term

### References

- [1] E.K. Akpınar and F. Koçyiğit, "Experimental investigation of thermal performance of solar air heater having different obstacles on absorber plates," International Communications in Heat and Mass Transfer, Vol. 37, pp. 416–421, 2010.
- [2] R. Karwa, S.C. Solanki and J.S. Saini, "Thermo-hydraulic performance of solar air heaters having integral chamfered rib roughness on absorber plates," Energy, Vol. 26, pp.161–176, 2001.
- [3] K.R. Aharwal, B.K. Gandhi and J.S. Saini, "Experimental investigation on heat-transfer enhancement due to a gap in an inclined continuous rib arrangement in a rectangular duct of solar air heater," Energy, Vol. 33, pp. 585–596, 2008.
- [4] A.M. Lanjewar, J.L. Bhagoria and R.M. Sarviyac, "Performance analysis of W-shaped rib roughened solar air heater," Journal of Renewable and sustainable energy, Vol. 3, pp. 043110, 2011.
- [5] K. Pottler, C.M. Sippel, A. Beck and J. Fricke, "Optimised finned absorber geometries for solar air heating collectors," Solar Energy, Vol. 67, pp. 35-52, 1999.
- [6] A. Priyam and P. Chand, "Thermal and thermohydraulic performance of wavy finned absorber solar air heater," Solar Energy, Vol. 130, pp. 250–259, 2016.
- [7] A.H. Falih, "Thermal Behavior in Dimple Square Duct with Inclined Perforated Baffles," Engineering and Technology Journal, Vol. 34, pp. 2047-2056, 2016
- [8] S. Chamoli and N. Thakur, "Performance study of solar air heater duct having absorber plate with V down perforated baffles," Songklanakarin J. Sci. Technol., Vol. 36, pp. 201-208, 2014.
- [9] R. Kumar, A. Kumar, R. Chauhan and M. Sethi, "Heat transfer enhancement in solar air channel with broken multiple V-type baffle," Case Studies in Thermal Engineering, Vol. 8, pp. 187–197, 2016.
- [10] A. Kumar and M.H. Kim, "Thermal Hydraulic Performance in a Solar Air Heater Channel with Multi V-Type Perforated Baffles," Energies, Vol. 9, pp. 564, 2016.
- [11] M.A. Karima and M.N.A. Hawlader, "Performance investigation of flat plate, v-corrugated and finned air collectors," Energy, Vol. 31, pp. 452–470, 2006.
- [12] S.V. Patanker, "Numerical heat transfer and fluid flow" McGraw-Hill, New York, 1980.

[13] B.T. Launder and D.B. Spalding, "Lecturers in Mathematical models of turbulence," Department of Mechanical Engineering, imperial college of Science and Technology, London, England, 1972.

[14] G. Fraisse, K. Johannes, V Berdal & G. Achard, "The use of a heavy internal wall with a ventilated air gap to store solar energy and improve summer comfort in timber frame houses," *Energy and Buildings*, vol. 38, pp: 293–302, 2006.

[15] J.M. Jalil, K.F. Sultan, L.A. Rasheed," Numerical and Experimental Investigation of Solar Air Collectors Performance Connected in Series," *Engineering and Technology Journal*, Vol. 35, pp. 190-196, 2017.

#### **Author(s) biography**



Prof. Dr. Jalal M. Jalil, University of Technology, Baghdad, Iraq, Electromechanical. Eng. Dept. Born in Iraq on 20 March 1945, Completed Bachelor of Engineering (Mechanical Engineering) in the year of 1980 and completed Master and PH.D of Engineering (Thermal Engineering) in the year of 1984 and 1988. His research area is heat transfer enhancement and renewable energy. E-mail: [jalalmjalil@gmail.com](mailto:jalalmjalil@gmail.com)